

# Pannexin1 is Expressed by Neurons and Glia but Does Not Form Functional Gap Junctions

YAN HUANG,<sup>1\*</sup> JUDITH B. GRINSPAN,<sup>2</sup> CHARLES K. ABRAMS,<sup>3</sup> AND STEVEN S. SCHERER<sup>1</sup>

<sup>1</sup>Department of Neurology, The University of Pennsylvania Medical Center, Philadelphia, Pennsylvania

<sup>2</sup>Research Neurology, Children's Hospital of Philadelphia, Philadelphia, Pennsylvania

<sup>3</sup>Department of Neuroscience and Neurology, Albert Einstein College of Medicine, Bronx, New York

## KEY WORDS

connexin; astrocytes; oligodendrocytes

## ABSTRACT

Pannexins are a newly described family of proteins that may form gap junctions. We made antisera against mouse pannexin1 (Panx1). HeLa cells expressing Panx1 have cell surface labeling, but not gap junction plaques, and do not transfer small fluorescent dyes or neurobiotin in a scrape-loading assay. *Neuro2a* cells expressing Panx1 are not electrophysiologically coupled. Intracellular Panx1-immunoreactivity, but not gap junction plaques, is seen in cultured oligodendrocytes, astrocytes, and hippocampal neurons. Thus, at least in these mammalian cells lines, Panx1 does not form morphological or functional gap junctions, and it remains to be demonstrated that Panx1 forms gap junction-forming protein in the CNS. © 2006 Wiley-Liss, Inc.

## INTRODUCTION

Gap junctions are channels that allow the diffusion of ions and small molecules between apposed cell membranes. Vertebrate gap junctions are formed by a family of molecules called connexins, comprised of about 20 different genes in mammals (Willecke et al., 2002). Six connexin molecules form a hemichannel and two apposed hemichannels form a functional channel. A different family of proteins, the innexins, form invertebrate gap junctions (Phelan et al., 1998a). Like connexins, innexins are predicted to have four transmembrane domains, with two extracellular loops and one intracellular loop, as well as N- and C-termini that are oriented similarly to connexins. Although they share an overall similarity, innexins do not appear to be homologous to connexins (Panchin, 2005; Phelan et al., 1998b).

Panchin et al. (2000) first described putative innexin homologs in different taxonomic groups. They identified three putative vertebrate innexins, which they termed pannexin1, 2, and 3 (Panx1, Panx2, and Panx3). Whether pannexins are orthologs of innexins, however, has been disputed (Barbe et al., 2006; White et al., 2004). Bruzzone et al. (2003) reported that neurons express Panx1 and Panx2 mRNA, whereas glia express Panx1 and not Panx2 mRNA, but others have failed to find glial expression of Panx1 mRNA (Ray et al., 2005; Vogt et al., 2005). In *Xenopus* oocytes, Panx1, but not Panx2, can form functional hemichannels; in paired oocytes, Panx1, alone and

with Panx2, forms functional channels, but Panx2 itself does not form functional channels (Bruzzone et al., 2003, 2005). Panx1 hemichannels are not gated by external  $Ca^{2+}$ , are remarkably sensitive to carbenoxolone, have large unitary conductance, are permeant for ATP, are mechanosensitive, and can be activated by extracellular ATP acting through P2Y purinergic receptors (Bao et al., 2004a; Bruzzone et al., 2005; Locovei et al., 2006a).

Here we describe our analysis of mouse Panx1 (mPanx1), using antisera raised against sequences in the C-terminus. mPanx1 is expressed in the cell membrane of transfected HeLa cells, but does not form gap junction plaques or functional channels in scrape-loading assays. Further, *Neuro2a* cells that express mPanx1 are not electrophysiologically coupled. Cultured oligodendrocytes, astrocytes, and hippocampal neurons express Panx1, which appears to be largely intracellular. Thus, at least in these mammalian cells lines, mPanx1 does not form functional homotypic gap junctions, and its role as a gap junction-forming protein in the CNS remains to be determined.

## MATERIALS AND METHODS

### Mouse Panx1 Expression Constructs

A primer (5'-TAAGTTTCATCCTCACATGTTTATTACCTCACACA-3') against a sequence from the 3' untranslated region of *mPanx1* (NCBI database BC049074) was used for reverse transcription of total RNA extracted from adult mouse cerebellum, using the Superscript First Strand Synthesis System (Invitrogen, Carlsbad, CA). The primers, 5'-CGGAATTCTTCGGCGTCTCGCCCCGGCT-3' and 5'-ATAAGAATGCGGCCGCTTACCTCACAAAACAAA-GCATCTTCCATGT-3', were used to amplify the entire open reading frame of *mPanx1*, adding *EcoRI* and *NotI* restriction sites to the 3' and 5' ends, respectively. The amplified fragment was digested with *EcoRI* and *NotI*,

This article contains supplementary material available via the Internet at <http://www.interscience.wiley.com/jpages/0894-1491/suppmat>.

Grant sponsor: National Institutes of Health; Grant number: RO1 NS42878, RO1 NS050705-01; Grant sponsor: Charcot-Marie-Tooth Association.

\*Correspondence to: Yan Huang, 464 Stemmler Hall, 36th Street and Hamilton Walk, The University of Pennsylvania Medical Center, Philadelphia, PA 19104-6077. E-mail: yan.huang.penn@gmail.com

Received 18 January 2006; Revised 18 August 2006; Accepted 22 August 2006

DOI 10.1002/glia.20435

Published online 28 September 2006 in Wiley InterScience (www.interscience.wiley.com).

cloned into pIRES-puro3 (Clontech, Mountain View, CA), and designated pIRES-puro3-mPannx1. The insert was sequenced, and found to be identical to BC049074. Using this construct as a template, a FLAG or EGFP tag was added to the C-terminus, designated pIRES-puro3-mPannx1-FLAG or pEGFP-N1-mPannx1, respectively. Mouse Pannx1 was also cloned into pIRES2-EGFP (Clontech); designated pIRES2-EGFP-mPannx1.

### Generation of Antisera

Two amino acid peptide sequences (1: IDGKIPTSLQTK-GEDQGSQRV; 2: EFKDLDSSEAAANNGEKNSRQ), corresponding to amino acids 377–397 and 398–419 of C-terminal region of mPannx1 (Supplemental Fig. 1), were selected for their immunogenicity using DSgene software (Accelrys, San Diego, CA). BLAST database searches showed that these sequences were unique to mPannx1. The peptide was synthesized by the Protein Resource Center of The Rockefeller University. Peptides were conjugated to keyhole limpet hemocyanin via a cysteine residue added at the C terminus during synthesis. Two rabbits were immunized to each peptide (Cocalico Biologicals, Reamstown, PA), and sera were screened by immunostaining and immunoblotting HeLa cells transiently transfected with pIRES-puro3-mPannx1. Three of four sera showed staining of transfected but not parental cells, and specific bands of appropriate size on immunoblots; these sera were designated 1859 (immunized with peptide 1), 1860, and 1861 (immunized with peptide 2) and were affinity-purified against the peptide immunogen immobilized on 1-mL columns prepared using SulfoLink (Pierce, Rockford, IL). The bound mPannx1 antibodies were eluted with 0.1 M glycine at pH 2.2 and immediately neutralized in 1/10 volume of 1 M Tris-Cl (pH 8.0), and then dialyzed overnight at 4°C in PBS containing 0.01% sodium azide. The affinity-purified antiserum (designated 1859-3p, 1860-3p, and 1861-3p; 3 indicates the third bleeding; p indicates affinity-purified) was again tested by immunostaining and immunoblotting HeLa cells transfected with pIRES-puro3-mPannx1 and on mouse or rat tissues. Of these three purified antiserum, 1860-3p gave the best signal and lowest background, and was the main one used in our experiments.

### Primary Cell Cultures

Cultures of oligodendrocyte precursors were established from the forebrains of 1-day-old C57BL/6J mice and seeded in serum-containing medium as previously described (Grinspan and Franceschini, 1995). After 1 day, the cells were switched to a serum-free growth medium until confluent (~1 week). To generate immature oligodendrocytes, oligodendrocyte precursors were removed from medium containing growth factors and fed with a “differentiation medium.” Cultures of primary astrocytes and neurons were prepared as previously described (Parpura et al., 1995; Wilcox and Dichter, 1994).

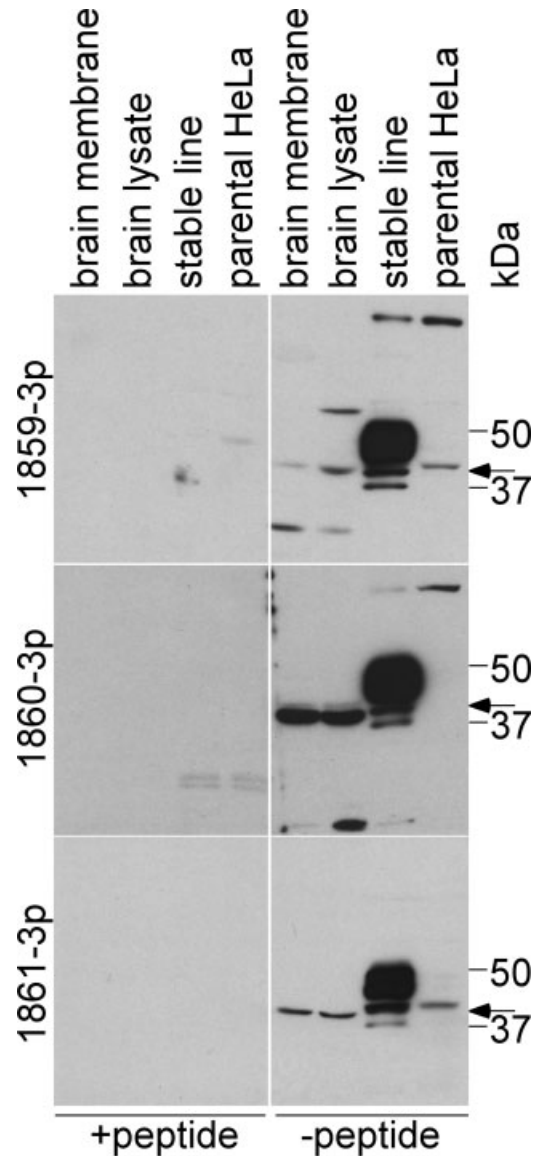


Fig. 1. Immunoblot analysis of rabbit antisera against mPannx1. These are images of immunoblots of brain lysates and brain membranes from adult mice, as well lysates of parental HeLa cells and HeLa cells that stably express mPannx1. Proteins were immunoblotted with one of three different affinity-purified rabbit antisera against one of two peptides derived from mPannx1. On the left side of each image, the cognate peptide was preincubated with the antiserum. All three antisera recognize several bands in transfected HeLa cells that are not present in parental HeLa cells, and a band ~40 kDa (arrow) in both brain lysates and brain membranes. 1859-3p and 1861-3p also recognized a least one band in parental HeLa cells that is similar in size to putative mPannx1.

### Cell Transfection

HeLa cells and COS7 cells were transiently transfected with pIRES-puro3-mPannx1 or pIRES-puro3-mPannx1-FLAG using Lipofectamine2000 (Invitrogen). Immunoblotting and immunostaining were performed 24–48 h after transfection. HeLa cells transfected with pIRES-puro3-mPannx1 were selected with 1  $\mu\text{g}/\mu\text{L}$  puromycin (Sigma-Aldrich). Single clones were screened for expression of

mPanx1 by immunostaining, and selected lines stably expressing mPanx1 were maintained in media supplemented with 1  $\mu\text{g}/\mu\text{L}$  puromycin. For electrophysiology (see later), *Neuro2a* cells were transfected with pEGFP-N1-mPanx1, pIRES2-EGFP-mPanx1, or empty vectors.

### Cell Surface Biotinylation

HeLa cells stably expressing mPanx1 were washed 3 times with PBS containing 0.1 mM  $\text{CaCl}_2$  and 1 mM  $\text{MgCl}_2$  (PBS+, pH 8.0), and all subsequent manipulations were conducted at 4°C. Cells were incubated with 2 mL of 0.5 mg/mL Sulfo-NHS-LC-Biotin (Pierce) in PBS+ for 30 min with gentle agitation, washed 5 times (10 min each) with 100 mM glycine in PBS+, and then lysed in 5 mM Tris-Cl (pH 7.6), 5 mM EDTA, 5 mM EGTA, 0.6% SDS, and 15 mM glycine supplemented with 1 mM phenylmethylsulfonyl fluoride (PMSF), 1  $\mu\text{g}/\text{mL}$  each of pepstatin A, leupeptin, and aprotinin (Sigma-Aldrich). The lysate was passed through a 22-gauge needle several times, incubated at 100°C for 3 min, passed through a 26-gauge needle 3 times, and centrifuged at 4°C for 10 min to harvest the supernatant, which was diluted with 2.5 volumes of IP buffer (100 mM NaCl, 20 mM sodium borate, 0.02%  $\text{NaN}_3$ , 15 mM EDTA, 15 mM EGTA (pH 8.2), 1.2% Triton X-100, 0.7% BSA). Twenty microliters of ImmunoPure-immobilized streptavidin beads (Pierce) was added to the diluted cell lysate, and rotated for 2 h at 4°C to bind the biotinylated proteins. The beads were washed 5 times with washing buffer (100 mM NaCl, 20 mM sodium borate, 0.02%  $\text{NaN}_3$ , 15 mM EDTA, 15 mM EGTA (pH 8.2), 0.5% Triton X-100, 0.1% SDS), and proteins were eluted by boiling in SDS-PAGE sample buffer (62.5 mM Tris-Cl (pH 6.8), 20% glycerol, 2% SDS, and 100 mM DTT). The eluted proteins as well as 30  $\mu\text{L}$  of their cognate unbound supernatant were separated on a 12% SDS-PAGE gel, and transferred to a polyvinylidene difluoride membrane. To confirm that the biotinylation reagent did not label intracellular proteins, the membrane was cut into two parts: one part was hybridized with the 1860-3p antiserum (1:1,000 dilution) and the other was hybridized with an antiserum against HSP90 (1:12,000 dilution; Santa Cruz Biotechnology, CA), as described later.

### Immunoblotting

Cell lysates were prepared using radioimmunoprecipitation assay buffer (10 mM sodium phosphate (pH 7.0), 150 mM sodium chloride, 2 mM EDTA, 50 mM sodium fluoride, 1% Nonidet P-40, 1% sodium deoxycholate, 0.1% SDS) supplemented with protease inhibitors (2 mM EDTA, 1 mM PMSF, and 1  $\mu\text{g}/\text{mL}$  pepstatin A, leupeptin, and aprotinin; Sigma-Aldrich). Tissue lysates were made by crushing snap-frozen tissues with a mortar and pestle on dry ice, suspending the powder in Tris-buffered SDS lysis buffer (50 mM Tris-Cl (pH 7.0), 1% SDS) and sonicated (Sonic Dismembrator; Fisher Scien-

tific, Pittsburgh, PA). Samples were spun at 4°C to pellet insolubles. Brain membranes were made from adult mice and rat at different ages. Animals were euthanized with  $\text{CO}_2$  gas, and the cerebrum, cerebellum, spinal cord, and optic nerves were rapidly dissected and placed in ice-cold PBS containing protease inhibitors (as earlier) and phosphatase inhibitor cocktail (Calbiochem, La Jolla, CA). Pooled brain regions were homogenized in ice-cold 0.32 M sucrose, 5 mM Tris-Cl (pH 7.4), and centrifuged for 10 min at 750g. The supernatants were isolated, sedimented for 60 min at 17,000g, and the resulting pellets were resuspended (in 1 mM EDTA, 5 mM Tris-Cl (pH 8.2)), homogenized, and placed on ice for 30 min. The lysate membranes were centrifuged 40 min at 27,000g, and the pellet was resuspended in 150 mM NaCl, 25 mM Tris (pH 7.4), and stored at  $-80^\circ\text{C}$ .

Protein concentrations were measured by a modified Lowry assay (BioRad, Hercules, CA). Fifty micrograms of protein was separated on a 12% SDS-PAGE gel, and transferred onto a polyvinylidene difluoride membrane. Membranes were blocked for 1 h with 5% powdered skim milk and 0.5% Tween 20 in PBS, and incubated overnight at 4°C with 1860-3p (1:1,000 dilution), a rabbit antiserum against HSP90 (1:12,000 dilution; Santa Cruz Biotechnology), or a mouse monoclonal antibody against the FLAG epitope tag (1:1,000 dilution; Sigma-Aldrich). After several washes, the blots were incubated in peroxidase-coupled secondary antibodies against rabbit or mouse IgG (1:10,000; Jackson ImmunoResearch, West Grove, PA) for 1 h at room temperature, washed several times, and developed using ECL plus (Amersham Biosciences, Arlington Heights, IL). To test the specificity of the affinity-purified rabbit anti-mPanx1 antisera, cognate peptides were preincubated with the corresponding antiserum at room temperature for 1 h, and then processed in parallel with antiserum incubated with a noncognate peptide or no peptide.

### Immunostaining

HeLa cells and primary glial cell cultures were fixed with acetone, blocked in 5% fish skin gelatin (in PBS) supplemented with 0.1% Triton X-100 at room temperature for 1 h, and incubated overnight at 4°C in different combinations with primary antibodies: 1860-3p (1:200 dilution), monoclonal antibodies against proteolipid protein (PLP; AA3 (Yamamura et al., 1991), 1:2 dilution), glial fibrillary acidic protein (GFAP; 1:400 dilution; Chemicon, Temecula, CA), connexin43 (1:400 dilution; Chemicon), or NeuN (1:100 dilution; Chemicon). Mice or rats of various ages were euthanized with  $\text{CO}_2$  gas according to University of Pennsylvania Institutional Care and Use Committee guidelines, and fixed by transcatheter perfusion with 4% paraformaldehyde in 0.1 M phosphate buffer (PB; pH 7.4). Dissected tissues were fixed for 60 min on ice, cryoprotected with infiltration in 20% sucrose in 0.1 M PB overnight, and embedded in OCT. Other mice or rats were euthanized and their unfixed tissues were immediately embedded in OCT. Cryostat sections (5–10  $\mu\text{m}$  thick) were thaw-

mounted on Super Frost Plus glass slides (Fisher Scientific, Pittsburgh, PA) and stored at  $-20^{\circ}\text{C}$ . Sections were permeabilized by immersion in  $-20^{\circ}\text{C}$  acetone for 10 min, blocked in 5% fish skin gelatin (in PBS) supplemented with 0.1% Triton X-100 at room temperature for 1 h, and incubated overnight at  $4^{\circ}\text{C}$  with primary antibodies—affinity-purified rabbit antiserum against anti-mPanx1 (1860-3p, 1:100 dilution), a mouse monoclonal antibody against GFAP (1:400 dilution; Chemicon), a mouse monoclonal antibody against NeuN (1:100 dilution; Chemicon), or a mouse monoclonal antibody against connexin47 (1:100 dilution; Invitrogen). The slides or coverslips were then washed several times and incubated with the appropriate fluorescein- and rhodamine-conjugated donkey cross-affinity-purified secondary antibodies (1:200 dilution; Jackson ImmunoResearch Laboratories). Slides were mounted with Vectashield (Vector Laboratories, Burlingame, CA), examined by epifluorescence with appropriate optical filters on a Leica (Nussloch, Germany) DMR light microscope, and photographed with a cooled Hamamatsu (Bridgewater, NJ) camera. The images were formatted with Adobe Photoshop (Adobe Systems, San Jose, CA). For the peptide blocking experiment, cognate peptides were preincubated with the mPanx1 antiserum at room temperature for 1 h, then diluted in the blocking buffer, and processed in parallel with untreated antiserum.

### Scrape Loading

HeLa parental cells and HeLa cells stably expressing human connexin26 (Cx26), human Cx43, “empty vector” (pIRESpuro3), or mPanx1 were grown on the 60-mm dishes. Cells were rinsed with PBS (without  $\text{CaCl}_2$  and  $\text{MgCl}_2$ ) before addition of the fluorescent dyes (final concentrations are given)—Lucifer Yellow (LY; 0.1%; Sigma-Aldrich), 5,6-carboxyfluorescein (0.8 mM; Sigma-Aldrich), ethidium bromide (5 mg/mL; Sigma-Aldrich), 4',6-diamidino-2-phenylindole (DAPI; 1 mg/mL; Sigma-Aldrich), TRITC-conjugated 10,000 kDa dextran (0.2%; Molecular Probes), and Neurobiotin (2%; Vector Laboratories, Burlingame, CA). The dyes were dissolved or diluted in PBS, added to the cells at room temperature, and the cells were cut with a carbon steel scalpel blade (Rib-back, Franklin Lakes, NJ). After 5 min, the slides were rinsed 3 times with PBS, then either examined immediately with an epifluorescence microscope or fixed in 4% paraformaldehyde in 0.1 M PB, washed, mounted with Vectashield (Vector Laboratories), and then imaged. For dye transfer of neurobiotin, cells were washed in HBSS, fixed with 4% paraformaldehyde, blocked with 5% fish skin gelatin with 0.1% Triton X-100 for 30 min at room temperature, incubated in Streptavidin–rhodamine (1:300 dilution; Invitrogen) for 60 min at room temperature, washed with PBS, and counterstained with DAPI. Images were taken and edited as described earlier.

### Electrophysiology

*Neuro2a* cells were transfected with pIRES2-EGFP vector, pIRES2-EGFP-mPanx1, or pIRES2-EGFP-Cx47.

Dual whole cell voltage clamping was performed as previously described (Abrams et al., 2003), using pipette solution (145 mM CsCl, 5 mM EGTA, 0.5 mM  $\text{CaCl}_2$ , 10 mM HEPES, pH 7.2) and bath solution (150 mM NaCl, 4 mM KCl, 1 mM  $\text{MgCl}_2$ , 2 mM  $\text{CaCl}_2$ , 5 mM dextrose, 2 mM pyruvate, 10 mM HEPES, pH 7.4). Junctional conductances were determined by measuring the instantaneous junctional currents in Cell 2 in response to Vj pulses from 0 to  $\pm 40$  or  $\pm 100$  mV in Cell 1 of an isolated cell pair and applying Ohm's Law. Cytoplasmic bridges were excluded by demonstrating the sensitivity of the junctional conductances to application of bath solution containing 2 mM octanol. Values are presented as mean  $\pm$  SEM. Differences in magnitudes were analyzed for statistical significance with the Kruskal–Wallis test with Dunn's multiple comparison tests. Frequencies of coupling were compared using Fisher's exact test.

## RESULTS

### Cloning mPanx1

There are two sequences reported to be mPanx1 in the NCBI database—AAH49074 (corresponding mRNA BC049074) and NP\_062355 (corresponding mRNA NM\_019482). We cloned mPanx1 cDNA from mouse brain by RT-PCR. This amplification generated a single band, and its deduced protein sequence exactly matched with that of AAH49074, which is more similar to both the human and the rat Panx1 sequences than is NP\_062355, which has a nonhomologous C-terminus owing to several mismatches, and especially an insertion of a single base that results in a frameshift. Another deduced mPanx1 sequence, Q9JIP4, was identical to AAH49074, except for a single nucleotide that would be predicted to alter an amino acid in the C-terminus.

### Generating and Characterizing mPanx1 Antisera

We immunized two rabbits each with one of two nonoverlapping peptides from the intracellular C-terminus (Supplemental Fig. 1)—the least homologous part of Panx1. In SDS-PAGE gels of HeLa cells (a human cell line), three of four of these crude antisera recognized “specific” bands, mostly in the 40–50 kDa range, in homogenates from transfected, but not from untransfected HeLa cells (data not shown). Affinity-purified antisera from these three antisera also recognized the same set of bands, most of which were slightly smaller than the predicted size of mPanx1 (48 kDa). Each affinity-purified antiserum also recognized at least one other band in parental HeLa cells; we considered these bands to be “non-specific,” but the band in the size range of mPanx1 seen by 1859 and 1861 could represent human Panx1, even though 12/21 and 11/22 of the amino acids of peptides 1 and 2 differ between mice and humans. All three affinity-purified antisera also labeled a  $\sim 40$  kDa band in lysates or membranes from adult mouse brain (arrow in Fig. 1); whether this is endogenous mPanx1 will be

discussed later. Preincubating each affinity-purified serum with its cognate peptide (Fig. 1), but not its noncognate peptide (data not shown), strongly attenuated the specific and the nonspecific bands. Similar results were found for transfected COS7 cells (a monkey cell line) in Supplemental Fig. 2, which also shows that the most prominent band is composed of at least two bands.

To provide additional evidence that our antisera recognize mPax1, we also made a FLAG-tagged mPax1 construct, in which the 11 amino acid FLAG epitope (DYKD DDDKAAA) was added to the C-terminus of mPax1. Duplicate blots were made from lysates of HeLa cells that had been transiently transfected with either the FLAG-tagged mPax1 or the nontagged mPax1 construct. One blot was hybridized with an affinity-purified rabbit antiserum against mPax1, and the other blot was hybridized with a mouse monoclonal antibody against FLAG. As shown in Fig. 2A, the rabbit Pax1 antiserum recognized both untagged and FLAG-tagged mPax1, but the signal of the higher molecular weight band(s) was conspicuously reduced when compared with its nontagged counterpart (compare Lanes 3 and 4). In addition, the FLAG tag appeared to increase slightly the apparent size of the smaller molecular weight band(s). The mouse anti-FLAG antibody only recognized the FLAG-tagged mPax1, and visualized relatively more of the higher molecular weight band(s) than did the rabbit anti-mPax1 antiserum (compare Lanes 7 and 3). We repeated this experiment 3 times with similar results, and used COS7 cells (data not shown), further demonstrating that expressing mPax1 expressed in HeLa cells produces multiple bands in the size range seen by the rabbit antisera.

We postulated that the FLAG tag inhibits the binding of the rabbit Pax1 antiserum to the adjacent peptide sequence, thereby accounting for the discrepancy between the visualization of larger species of FLAG-tagged mPax1 with these two different antibodies. To address this issue, we immunoprecipitated lysates of HeLa cells transiently transfected with FLAG-tagged mPax1 with either the mouse anti-FLAG antibody or the affinity-purified rabbit antiserum (1860-3p), and hybridized the immunoprecipitated proteins with the 1860-3p or the mouse anti-FLAG antibody, respectively. As shown in Fig. 2B, the lower band(s) was immunoprecipitated by both antibodies, whereas the mouse anti-FLAG antibody immunoprecipitated relatively more of the higher molecular weight band(s) than did the rabbit Pax1 antiserum. These data support the idea that the FLAG epitope diminished the binding of the rabbit antiserum to the larger band(s) of FLAG-tagged mPax1, and provide further evidence that our antisera recognizes mPax1. We were unable, however, to immunoprecipitate mPax1 from brain extracts (data not shown).

### mPax1 Does Not Form Gap Junction Plaques

To localize mPax1, we immunostained transiently transfected as well as bulk selected HeLa cells stably expressing mPax1. All three affinity-purified antisera

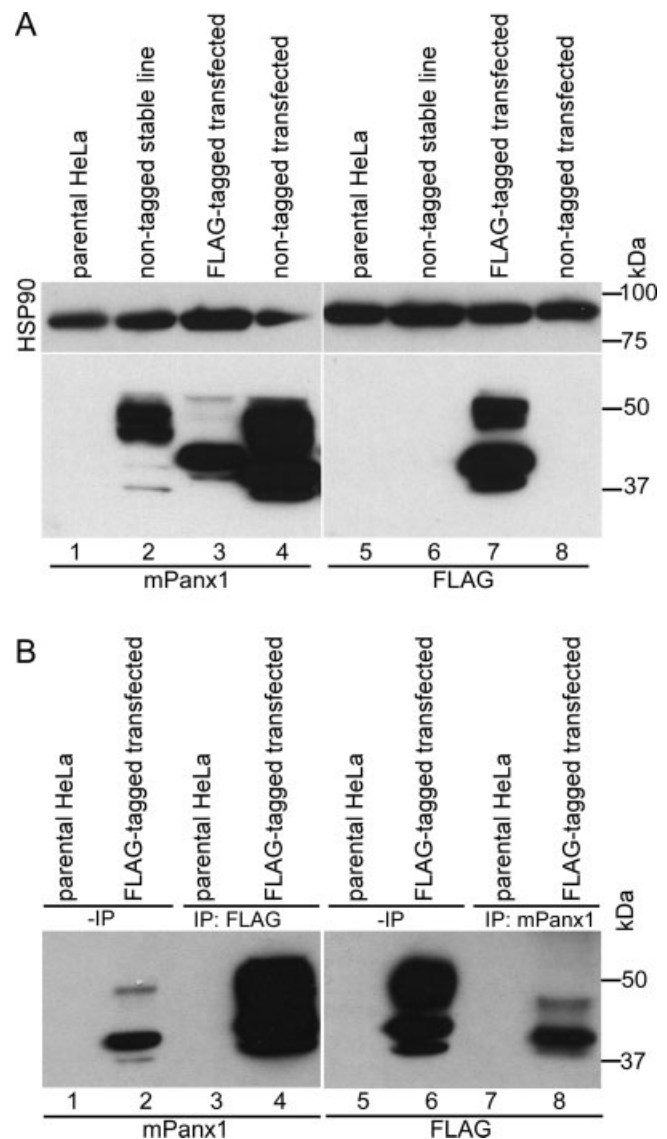


Fig. 2. Immunoblot and immunoprecipitation of mPax1 and FLAG-tagged mPax1. **A**. These are images of immunoblotted lysates from parental HeLa cells, HeLa cells that stably express mPax1, or HeLa cells that were transiently transfected to express FLAG-tagged or nontagged mPax1. Duplicate blots were prepared and split; the upper portion was hybridized with a rabbit antiserum against HSP90 (demonstrating comparable loading of each sample); the lower portion was hybridized with an affinity-purified rabbit antiserum against mPax1 (1860-3p) or a mouse monoclonal antibody against FLAG, as indicated. Note that the Pax1 and FLAG antibodies label bands of comparable sizes; that FLAG tag appeared to increase slightly the apparent size of the smaller molecular weight bands (compare Lanes 3 and 4); that the mouse anti-FLAG antibody only recognized the FLAG-tagged mPax1, and visualized relatively more of the higher molecular weight band(s) when compared with the anti-mPax1 antiserum (compare Lanes 7 and 3). **B**. These are images of immunoprecipitates from cells that were transiently transfected to express FLAG-tagged mPax1. Lysates were either immunoprecipitated with a mouse anti-FLAG monoclonal antibody, then hybridized with an affinity-purified rabbit antiserum against mPax1 (1860-3p, left panel), or immunoprecipitated with an affinity-purified rabbit antiserum against mPax1 (1860-3p), and then hybridized with the FLAG antibody (right panel). Cell lysates (Lanes 1, 2 and 5, 6) were included for comparison. Note that the lower band(s) was immunoprecipitated by these two antibodies, whereas the upper band(s) was more efficiently being immunoprecipitated by FLAG antibody (compare Lanes 4 and 8).

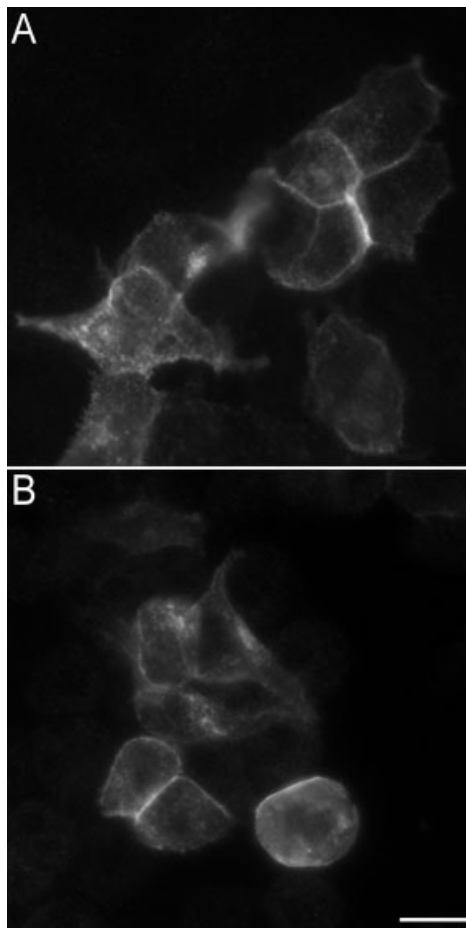


Fig. 3. mPanx1 does not form gap junction plaques in HeLa cells. These are images of HeLa cells that were transiently transfected with the mPanx1 construct (A) or bulk selected HeLa cells that stably express mPanx1 (B). The cells were immunostained with an affinity-purified rabbit antiserum against mPanx1 (1860-3p). Note that mPanx1-immunoreactivity outlines cells, especially at apposed cell membranes, but gap junction plaques are not seen. Scale bar: 10  $\mu$ m.

stained a subset of cells, including the cell membrane (this was particularly evident at apposed cell membranes), whereas parental cells showed no such staining (Fig. 3; data not shown). Although mPanx1 has been reported to form functional channels when expressed in *Xenopus* oocytes (Bruzzone et al., 2003), we did not observe typical gap junction plaques between adjacent mPanx1-positive HeLa cells. When compared with HeLa cells expressing nontagged mPanx1, transiently transfected cells expressing FLAG-tagged mPanx1 showed less prominent Panx1 labeling at their cell membranes, and more prominent intracellular staining that colocalized with an ER marker; as seen with either a mouse anti-FLAG antibody (data not shown) or a rabbit anti-mPanx1 antiserum (Supplemental Figs. 3A–C). HeLa cells expressing EGFP-tagged mPanx1 had intracellular staining (data not shown); some cells had large, intracellular aggregates that could be observed directly owing to the EGFP tag itself (data not shown) or by immunostaining with an antiserum to mPanx1 (Supplemental Fig. 3D).

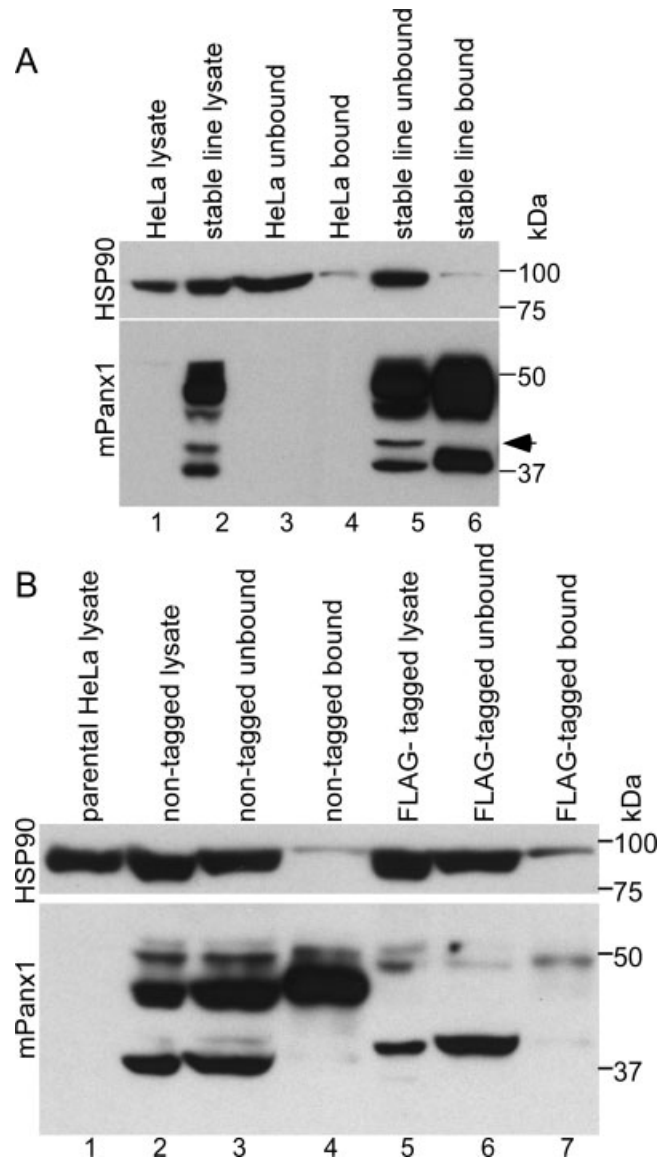
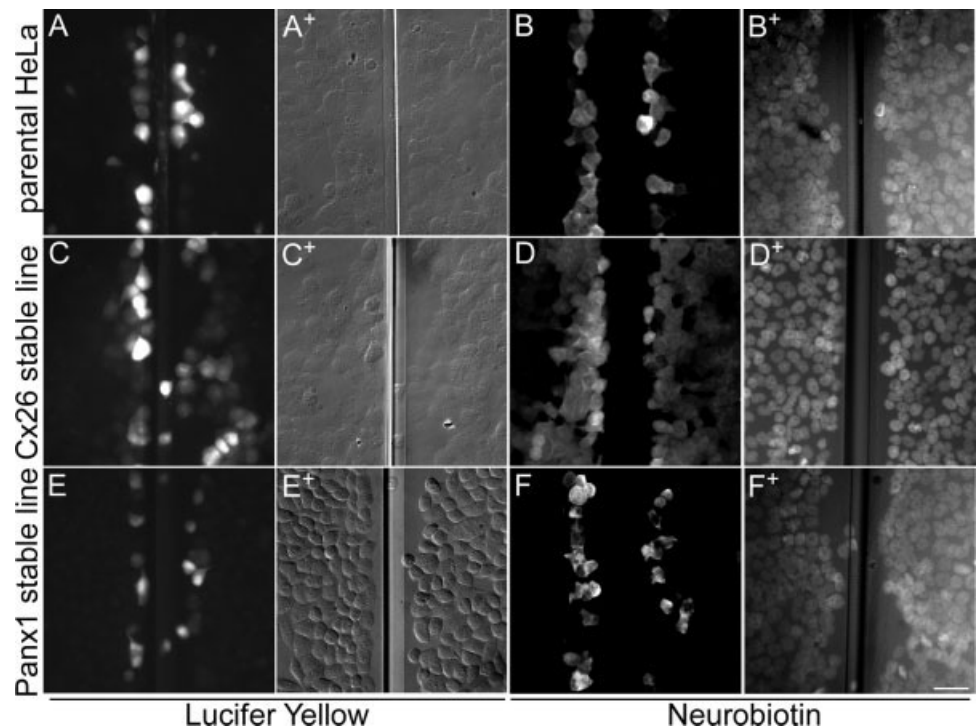


Fig. 4. Cell-surface biotinylation of mPanx1 in HeLa cells. The cell-surface proteins of parental HeLa cells and cells stably expressing mPanx1 (A) and transiently transfected HeLa cells (B) were biotinylated. The biotinylated (bound) and “unbound” proteins were immunoblotted, along with lysates. After transfer, the membrane was cut into two pieces; the lower piece was hybridized with an affinity-purified rabbit antiserum against mPanx1 (1860-3p), and the upper piece was hybridized with a rabbit antiserum against HSP90. In HeLa cells stably expressing mPanx1 (A), note that the similar appearance of the bound/biotinylated fraction (Lane 6), the unbound/nontinylated fraction (Lane 5), and the HeLa lysates (Lane 2); only one band (arrow) does not appear to have been biotinylated. In transiently transfected cells (B), note that the larger band(s) was relatively more biotinylated for both untagged (Lane 4) and FLAG-tagged (Lane 7) mPanx1 than the corresponding unbound fractions (Lanes 3 and 6). In both A and B, there was relatively little labeling of HSP90 in the bound portion when compared with the unbound portion.

To determine whether mPanx1 reached the cell membrane, we performed cell-surface biotinylation on intact cells. Biotinylated proteins were recovered with avidin (the “bound” fraction), and compared with the “unbound” fraction and bulk cell lysates. In HeLa cells stably expressing mPanx1, all but one of the Panx1 bands were

Fig. 5. mPanx1 does not form functional gap junction channels in HeLa cells. These are images of scrape-loaded parental HeLa cells, as well as HeLa cells stably expressing human Cx26 or mPanx1. Panels A, C, and E show cells labeled with Lucifer Yellow (LY); A+, C+, and E+ are the corresponding phase contrast images. Panels B, D, and F show cells labeled with neurobiotin (NB) and visualized with rhodamine-conjugated avidin; B+, D+, and F+ are the corresponding images showing the nuclei stained with DAPI. Note that cells stably expressing Cx26 show dye transfer with both LY and NB, whereas parental HeLa cells and cells stably expressing mPanx1 do not show dye transfer. Scale bar: 30  $\mu$ m.



biotinylated (indicated by the arrowhead in Fig. 4A). In transiently transfected HeLa cells, however, the larger mPanx1 band was preferentially biotinylated (compare Lanes 3 and 4 in Fig. 4B). Thus, the robust biotinylation of mPanx1, in contrast to an intracellular protein HSP90, demonstrates that mPanx1 reached the cell membrane. In contrast, relatively little FLAG-mPanx1 was biotinylated (Fig. 4B), consistent with its apparent retention in the ER (Supplemental Fig. 3). These experiments were repeated several times with similar results.

### mPanx1 Does Not Form Functional Gap Junctions

To determine whether mPanx1 formed functional gap junctions, we “scrape loaded” HeLa cells that stably expressed mPanx1. In this assay (El-Fouly et al., 1987; Trosko et al., 2000), a confluent monolayer of cells is injured with a scalpel blade in media containing a small molecule, usually a fluorescent dye, that can be visualized. We found no transfer with four different fluorescent dyes—Lucifer Yellow (LY, MW 457; Fig. 5 and Supplemental Fig. 4), ethidium bromide (MW 394; data not shown), 5,6-carboxyfluorescein (MW 376; data not shown), and DAPI (MW 457; data not shown), or with Neurobiotin (MW 287)—which itself is not fluorescent, but can be visualized because it binds to TRITC-conjugated avidin (Fig. 5). No dye transfer was found in HeLa parental cells, whereas HeLa cells stably expressing human Cx26 showed transfer with all dyes (Fig. 5; data not shown). These experiments were done at least 5 times for LY and Neurobiotin, 3 times for carboxyfluorescein, and twice for ethidium bromide, DAPI, and the combination of Neurobiotin and TRITC-conjugated dextran.

To study this issue more definitively, we performed electrophysiology in *Neuro2a* cells. *Neuro2a* cells are easier to record than HeLa cells, and also have extremely low endogenous junctional coupling (Fig. 6), making them an ideal cell type for confirming the absence of even low levels of electrical coupling. Cells were transfected with the pIRES2-EGFP-mPanx1 construct, in which EGFP is expressed from an internal ribosome entry site (IRES). This vector allowed us to identify cells likely to express mPanx1; we demonstrated this directly by showing that all cells expressing EGFP were mPanx1-positive (data not shown). For comparison, we also transfected *Neuro2a* cells with pIRES2-Cx47, which forms functional gap junctions (Abrams, unpublished observations). As summarized in Fig. 6, all Cx47 expressing pairs were highly coupled, while a minority of mPanx1 expressing pairs were coupled, at low levels not significantly different than those in cells transfected with the pIRES2-EGFP vector alone. In addition, the characteristics of this low level coupling are similar to those seen between untransfected *Neuro2a* cells (Abrams, unpublished observations). Statistical analysis showed no significant differences in the magnitude or the frequency of coupling between pIRES2-EGFP-mPanx1 transfected cells and pIRES2-EGFP transfected cells, while significant differences were found between pIRES2-EGFP-Cx47 transfected cells and pIRES2-EGFP-mPanx1/pIRES2-EGFP transfected cells. Thus, in contrast to *Xenopus* oocytes (Bruzzone et al., 2003), our data indicate that mPanx1 does not form functional gap junctions in *Neuro2a* cells. *Neuro2a* cells transfected with pEGFP-N1-mPanx1 construct (EGFP is fused with the C-terminus of mPanx1) exhibited a similar lack of coupling (data not shown).

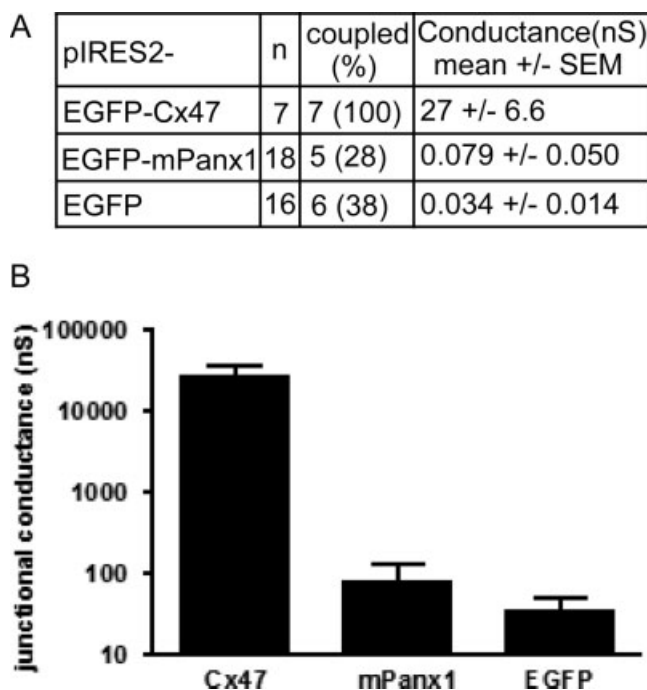


Fig. 6. mPanx1 does not form functional gap junctions in *Neuro2a* cells. Junctional conductance between pairs of *Neuro2a* cells transfected with human Cx47, mPanx1, or vector alone are tabulated (A) and shown graphically (B). All Cx47 expressing pairs were highly coupled, while a minority of mPanx1 cells were coupled, and at low levels similar to that in cells transfected with vector alone. Neither the magnitude nor the frequency of coupling was significantly different between cells expressing mPanx1 versus vector alone; both characteristics were significantly different in cells expressing Cx47.

**Panx1 is Expressed in Cultured Astrocytes, Oligodendrocytes, and Hippocampus Neurons**

There are conflicting results regarding what cells express Panx1. Bruzzone et al. (2003) reported that neurons and glia express Panx1 mRNA, but Ray et al. (2005) and Vogt et al. (2005) failed to find glial expression. To examine this question, we immunoblotted and immunostained primary cultures of mouse astrocytes, rat hippocampal neurons, and mouse oligodendrocytes (differentiated for 5 days), as well as selected tissues of adult mice. All three affinity-purified antisera against mPanx1 labeled band(s) about the size of mPanx1 (Fig. 7A; data not shown) in lysates from each of these cell cultures, and in multiple regions of CNS; no signal was detected in kidney, heart, or skeletal muscle (Supplemental Fig. 5A). Similar results were found with the 1859-3p and 1861-3p antisera (Supplemental Fig. 5B and C).

Vogt et al. (2005) reported that the expression of mPanx1 mRNA in mouse CNS peaked around P1 and then progressively decreased. To determine whether the mPanx1 protein had the same expression profile, we immunoblotted lysates of cerebrum, cerebellum, and spinal cord from P1, P10, P20, P30, and P90 rats with an affinity-purified antiserum (1860-3p). In the spinal cord (Fig. 7B, right panel) and cerebellum (not shown), the levels of Panx1 decreased during development, but this trend was less evident in the cerebrum, in which Panx1 appeared to decrease later (Fig. 7B, left panel). To determine the cellular localization of Panx1, we immunostained frozen sections of mouse and rat spinal cord, cerebellum, and brain. In spite of numerous attempts on both unfixed and fixed tissue, we did not observe a consistent pattern of immunostaining with the three different affinity-purified antisera, including the two (1860-3p

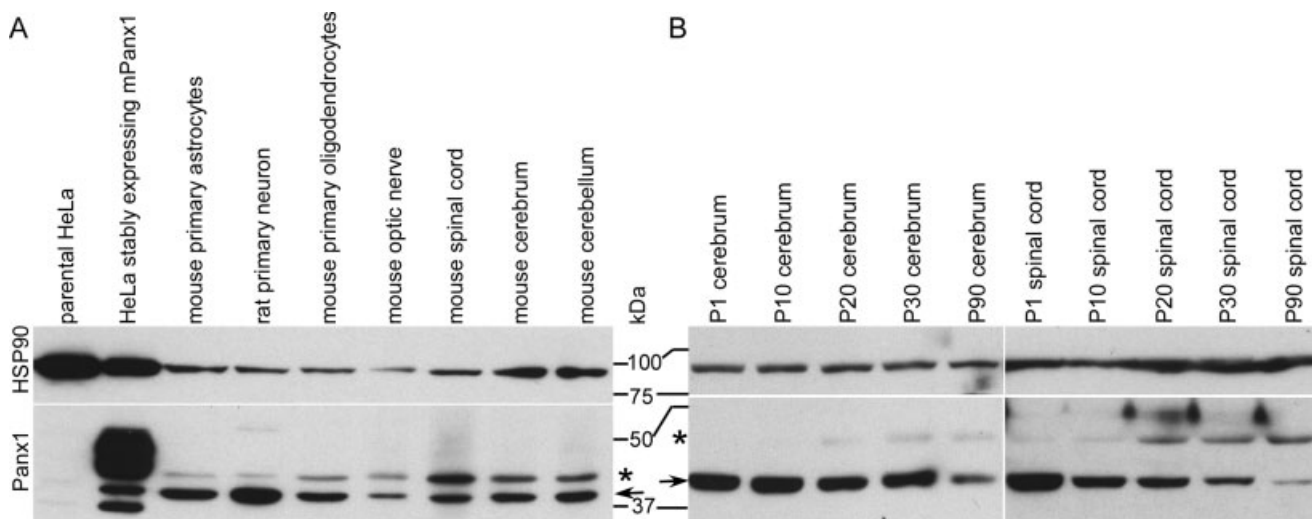


Fig. 7. Panx1 is expressed by multiple cells and tissues. These are images of immunoblots of lysates from the indicated cells/tissues. The membranes were cut into two pieces; one was hybridized with an affinity-purified rabbit antiserum against mPanx1 (1860-3p, lower panels) and the other with a rabbit antiserum against HSP90 (upper panels). Cultures of primary astrocytes, neurons, and oligodendrocytes, as well as

adult rat optic nerve, spinal cord, cerebrum, and cerebellum all showed two bands (marked by an asterisk and an arrow) ~40 and 45 kDa; these bands are in the size range of those in transfected HeLa cells (A). The amount of the lower band decreased from postnatal day 1 (P1) to P90 in the rat cerebrum and spinal cord (arrow); the amount of the upper band (asterisk) appeared to increase with age (B).

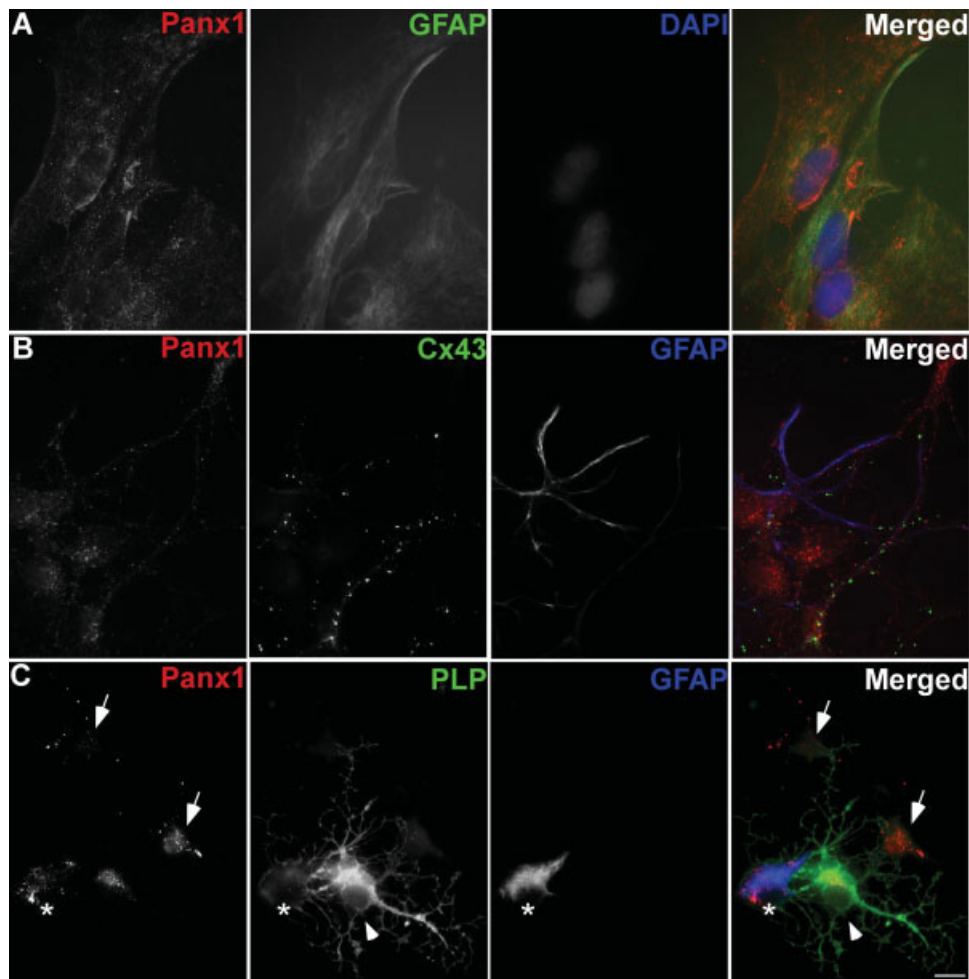


Fig. 8. Cultured astrocytes, hippocampal neurons, and oligodendrocytes express Panx1. These are images of primary cultures of astrocytes (A), hippocampal neurons (B), and oligodendrocytes (C) immunostained with an affinity-purified rabbit antiserum against mPanx1 (1860-3p), combined with monoclonal antibodies against glial fibrillary acidic protein (GFAP), Cx43, or PLP, and the nuclear counterstain DAPI, as indicated. Astrocytes (A), neurons (B), PLP-negative, immature

oligodendrocytes (C; arrow), PLP-positive/mature oligodendrocytes (C; arrowhead), and GFAP-positive “Type 2 astrocytes” (C; asterisk) were all Panx1-positive. Note that Panx1 is localized in both the cell body and processes in the immature oligodendrocytes, but only in the cell body of the mature oligodendrocyte (C; arrowhead), and that Panx1 does not colocalize with Cx43, the main connexin expressed by astrocytes (B). Scale bar: 10  $\mu$ m.

and 1861-3p) that were raised against the same peptide sequence; the other antiserum (1859-3p) labeled all cellular elements in a diffuse pattern that we interpreted as background staining (data not shown). Given these results, resolving the cellular localization in vivo may require comparing wild type and *Panx1*-null mice.

As an alternative approach, we immunostained primary cultures of neurons, astrocytes, and oligodendrocytes with the same three affinity-purified antisera. We observed a consistent pattern of staining with the two antisera against the more distal peptide (1860-3p and 1861-3p): there were puncta of Panx1-immunoreactivity that appeared to be largely localized in the cytoplasm of all three cell types (Fig. 8); the antiserum against the other peptide (1859-3p) showed a high level of diffuse staining that we interpreted as background staining (data not shown). We confirmed the cellular identity of the Panx1-positive cells by double/triple-labeling them with monoclonal antibodies against the astrocytic mar-

kers GFAP (Fig. 8A), Cx43 (Fig. 8B), the neuronal marker NeuN (data not shown and Supplemental Fig. 6), and PLP, a marker of mature oligodendrocytes (Fig. 8C). In oligodendrocyte cultures, the Panx1 antisera labeled small, round, process-bearing cells that are known to be immature oligodendrocytes (Grinspan and Franceschini, 1995), which we were able to label with the monoclonal antibody A2B5 (data not shown), which binds to glycolipids expressed by these cells (Farrer and Quarles, 1999). The Panx1-positive puncta seen with 1860-3p and 1861-3p were abolished by preincubation with the cognate peptide (Supplemental Fig. 6). To determine whether Panx1 is incorporated into the cell membrane of astrocytes or neurons, we performed cell-surface biotinylation on intact cells. No biotinylated Panx1 protein was detected in cultures of astrocytes or hippocampal neurons (Fig. 9). These experiments were repeated once with similar results, and indicated that Panx1 is not localized to the cell membranes of cultured astrocytes or neurons.

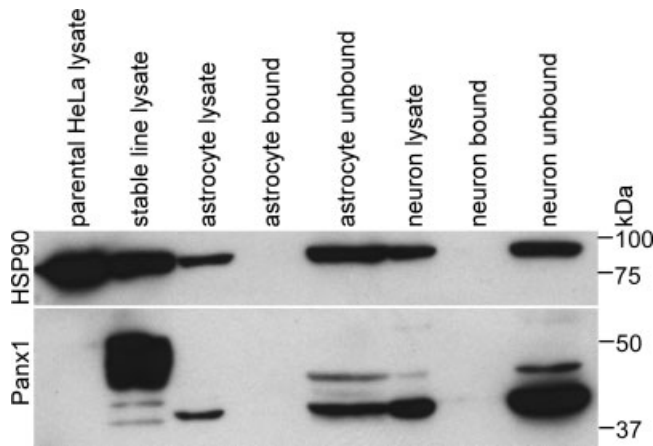


Fig. 9. No cell-surface biotinylated Panx1 in primary astrocytes and hippocampal neurons. Cell-surface biotinylated (bound) and unbound proteins of astrocytes and hippocampal neurons were separated on a SDS-PAGE gel, along with lysates of astrocytes, neurons, parental HeLa cells, and HeLa cells that stably express mPanx1. After transfer, the membrane was cut into two pieces; the lower piece was hybridized with an affinity-purified rabbit antiserum against mPanx1 (1860-3p) and the upper piece was hybridized with a rabbit antiserum against HSP90. Biotinylated (bound) Panx1 was not detected in either astrocytes or hippocampal neurons, but bands corresponded to mPanx1 (in HeLa cells expressing mPanx1) were seen in both the lysates and unbound samples from astrocytes and neurons.

## DISCUSSION

### Multiple Panx1 Bands in Transfected Cells

We characterized three different antisera against one of two different peptides derived from mPanx1. All three antisera recognized a similar set of bands in transfected cells, as did an antibody against FLAG-tagged mPanx1. These results are similar to recent reports in which immunoblots of transfected cells expressing Panx1 gives multiple bands, the size of which depends on the epitope tag—estimated to be ~48 kDa without a tag (Zappala et al., 2006), ~40–45 kDa with a myc tag (Bruzzone et al., 2005), and ~75 kDa with a EGFP tag (Dvorianchikova et al., 2006). Panx1 antisera have been reported to label ~43 kDa band in mouse tissues (Dvorianchikova et al., 2006) and human erythrocytes (Locovei et al., 2006b), and a ~48 kDa band in brain homogenates (Zappala et al., 2006). Our Panx1 antisera also recognized one or two bands in the same size range in various brain regions, and these putative Panx1 bands were abolished by incubating the sera with their cognate peptide. Thus, it is highly likely that our antisera recognize endogenous mPanx1, which appears to be smaller than the predominant band found in transfected cells. It is possible that our antisera also recognize human and monkey Panx1, in HeLa and COS7 cells, respectively, but this does not affect our results.

Why are multiple Panx1 bands seen in lysates of transfected cells? Neither our RT-PCR results, nor a search of the NCBI database revealed any alternatively spliced forms of mPanx1, so we considered the possibility that Panx1 might be posttranslationally modified. We did not find any consensus sites for N-linked glycosylation (the one mentioned by Dvorianchikova et al. (2006) is

not because it is intracellular), but the NetPhos 2.0 program (<http://www.cbs.dtu.dk/services/NetPhos/>) predicts that many intracellular amino acids could be phosphorylated (6 serines, 3 tyrosines, and 1 threonine). To test the possibility that the multiple bands represent different degrees of phosphorylation, we followed a dephosphorylation protocol previously used to demonstrate that Cx43 is phosphorylated (Bao et al., 2004b; Musil et al., 1990), but our results were inconclusive. In transiently transfected cells, the larger mPanx1 bands appeared to be preferentially biotinylated, but this result was not confirmed in stably expressing cells. Thus, the basis of the multiple bands of Panx1 in transfected cells remains to be determined.

### Pannexin1 Did Not Form Functional Gap Junctions

When expressed in HeLa cells, mPanx1 is found on the cell membrane, as shown by immunostaining and cell-surface biotinylation. Gap junction plaques (puncta of intense staining that are localized at the borders of adjacent cells), however, were not found. The lack of plaques suggested that mPanx1 does not form functional gap junctions, as plaques are typically present in cells that express connexins that form functional gap junctions, Cx26, Cx30, Cx30.3, Cx31, Cx32, Cx36, Cx37, Cx40, Cx43, Cx45, Cx46, and Cx50 (Elfgang et al., 1995; Kleopa et al., 2002; Plantard et al., 2003; Teubner et al., 2000; White, 2002; Yeh et al., 1998), but not in cells that express Cx29 (Scherer, unpublished), which does not form functional gap junctions (Altevogt et al., 2002). In keeping with this suggestion, we found no evidence of functional gap junctions by scrape-loading HeLa cells that stably expressed mPanx1, or by electrophysiological recordings of *Neuro2a* cell-pairs expressing mPanx1. These results contrast with the ability of Panx1 to form homotypic gap junctions in *Xenopus* oocytes (Bruzzone et al., 2003, 2005). This contradiction has been noted for some Cx32 mutants (Met34Val, Arg75Gln, Arg164Trp, Cys217x), which form functional gap junctions in oocytes, whereas they appear to be retained intracellular in mammalian cells (Oh et al., 1997; Wang et al., 2004; Yum et al., 2002). Perhaps, oocytes contain another pannexin that interacts with Panx1 to form functional channels. Another possibility is that posttranslational modification of mPanx1 in HeLa and *Neuro2a* cells abolishes its ability to form functional channels, akin to how phosphorylation diminishes the function of Cx43 channels (Bao et al., 2004b; Musil et al., 1990). The reason for this discrepancy remains to be resolved.

### Neurons and Glia Express Panx1

By situ hybridization, neurons are the preponderant cell type expressing Panx1 and Panx2 in the CNS (Bruzzone et al., 2003; Ray et al., 2005; Vogt et al., 2005), leading to the proposal that Panx1 and Panx2 form electrical synapses. Panx1-immunoreactivity is mainly intracellular; the published images do not adequately document the claim of cell surface expression (Dvorianchi-

kova et al., 2006; Zappala et al., 2006). We found that neuronal staining at least in the cell soma appeared intracellular, and the lack of cell surface labeling by biotinylation goes against the idea that Panx1 forms neuronal channels (Simon et al., 2005; Vogt et al., 2005) or hemichannels (Thompson et al., 2006). The localization of Panx1 in vivo needs further study, which would be greatly facilitated by the generation of a *Panx1*-null mouse.

Whether glia also express Panx1 mRNA has been disputed. Bruzzone et al. (2003) found in labeling in the white matter in an unidentified population of cells, whereas Ray et al. (2005) and Vogt et al. (2005) did not find Panx1 mRNA in white matter, and in the gray matter, Panx1 mRNA was associated with neurons and not GFAP-positive astrocytes. Antibody staining indicate that, with the exception for the Bergmann glia of the cerebellum, Panx1-immunoreactivity appears to be exclusively expressed by neurons (Dvorianchikova et al., 2006; Zappala et al., 2006). Our data indicates that cultured astrocytes and immature oligodendrocytes express mPanx1 protein, with the caveat that Panx1 expression in cultured cells may not mirror Panx1 expression in vivo.

#### ACKNOWLEDGMENTS

The authors thank Dr. Linda Musil for advice, Dr. Sabrina Yum for the HeLa cells that stably express Cx26, Margaret Maronski for the primary neurons, and Elizabeth Stambrook for the cultured astrocytes.

#### REFERENCES

- Abrams CK, Freidin M, Bukauskas F, Dobrenis K, Bargiello TA, Verselis VK, Bennett MVL, Chen L, Sahenk Z. 2003. Pathogenesis of X-linked Charcot-Marie-Tooth disease: Differential effects of two mutations in connexin 32. *J Neurosci* 23:10548–10558.
- Altevogt BM, Kleopa KA, Postma FR, Scherer SS, Paul DL. 2002. Cx29 is uniquely distributed within myelinating glial cells of the central and peripheral nervous systems. *J Neurosci* 22:6458–6470.
- Bao L, Locovei S, Dahl G. 2004a. Pannexin membrane channels are mechanosensitive conduits for ATP. *FEBS Lett* 572:65–68.
- Bao XY, Altenberg GA, Reuss L. 2004b. Mechanism of regulation of the gap junction protein connexin 43 by protein kinase C-mediated phosphorylation. *Am J Physiol Cell Physiol* 286:C647–C654.
- Barbe MT, Monyer H, Bruzzone R. 2006. Cell–cell communication beyond connexins: The pannexin channels. *Physiology* 21:103–114.
- Bruzzone R, Barbe MT, Jakob NJ, Monyer H. 2005. Pharmacological properties of homomeric and heteromeric pannexin hemichannels expressed in *Xenopus* oocytes. *J Neurochem* 92:1033–1043.
- Bruzzone R, Hormuzdi SG, Barbe MT, Herb A, Monyer H. 2003. Pannexins, a family of gap junction proteins expressed in brain. *Proc Natl Acad Sci USA* 100:13644–13649.
- Dvorianchikova G, Ivanov D, Panchin Y, Shestopalov VI. 2006. Expression of pannexin family of proteins in the retina. *FEBS Lett* 580:2178–2182.
- Elfgang C, Eckert R, Lichternberg-Frate H, Butterweck A, Traub O, Klein RA, Hulser DF, Willecke K. 1995. Specific permeability and selective formation of gap junction channels in connexin-transfected HeLa cells. *J Cell Biol* 129:805–817.
- El-Fouly M, Trosko J, Chang C. 1987. Scrape-loading and dye transfer. A rapid and simple technique to study gap junctional intercellular communication. *Exp Cell Res* 168:422–430.
- Farrer RG, Quarles RH. 1999. GT3 and its O-acetylated derivative are the principal A2B5-reactive gangliosides in cultured O2A lineage cells and are down-regulated along with O-acetyl GD3 during differentiation to oligodendrocytes. *J Neurosci Res* 57:371–380.
- Grinspan JB, Franceschini B. 1995. PDGF is a survival factor for PSA-NCAM+ oligodendroglial pre-progenitor cells. *J Neurosci Res* 41:540–551.
- Kleopa KA, Yum SW, Scherer SS. 2002. Cellular mechanisms of connexin32 mutations associated with CNS manifestations. *J Neurosci Res* 68:522–534.
- Locovei S, Bao L, Dahl G. 2006a. Activation of pannexin 1 channels by ATP through P2Y receptors and by cytoplasmic calcium. *FEBS Lett* 580:239–244.
- Locovei S, Bao L, Dahl G. 2006b. Pannexin 1 in erythrocytes: Function without a gap. *Proc Natl Acad Sci USA* 103:7655–7659.
- Musil LS, Cunningham BA, Edelman GM, Goodenough DA. 1990. Differential phosphorylation of the gap junction protein connexin43 in junctional communication-competent and -deficient cell lines. *J Cell Biol* 111:2077–2088.
- Oh S, Ri Y, Bennett MVL, Trexler EB, Verselis VK, Bargiello TA. 1997. Changes in permeability caused by connexin 32 mutations underlie X-linked Charcot-Marie-Tooth disease. *Neuron* 19:927–938.
- Panchin YV. 2005. Evolution of gap junction proteins—The pannexin alternative. *J Exp Biol* 208:1415–1419.
- Panchin Y, Kelmanson I, Matz M, Lukyanov K, Usman N, Lukyanov S. 2000. A ubiquitous family of putative gap junction molecules. *Curr Biol* 10:R473, R474.
- Parpura V, Liu F, Brethorst S, Jeftinija K, Jeftinija S, Haydon PG. 1995.  $\alpha$ -Latrotoxin stimulates glutamate release from cortical astrocytes in cell culture. *FEBS Lett* 360:266–270.
- Phelan P, Stebbings LA, Baines RA, Bacon JP, Davies JA, Ford C. 1998a. *Drosophila* shaking-B protein forms gap junctions in paired *Xenopus* oocytes. *Nature* 391:181–184.
- Phelan P, Bacon JP, Davies JA, Stebbings LA, Todman MG, Avery L, Baines RA. 1998b. Innexins: A family of invertebrate gap-junction proteins. *Trends Genet* 14:348, 349.
- Plantard L, Huber M, Macari F, Meda P, Hohl D. 2003. Molecular interaction of connexin 30.3 and connexin 31 suggests a dominant-negative mechanism associated with erythrokeratoderma variabilis. *Hum Mol Genet* 12:3287–3294.
- Ray A, Zoidl G, Weickert S, Wahle P, Dermietzel R. 2005. Site-specific and developmental expression of pannexin1 in the mouse nervous system. *Eur J Neurosci* 21:3277–3290.
- Simon AM, Olah S, Molnar G, Szabadics J, Tamas G. 2005. Gap-junctional coupling between neurogliaform cells and various interneuron types in neocortex. *J Neurosci* 25:6278–6285.
- Teubner B, Degen J, Sohl G, Guldenagel M, Bukauskas F, Trexler E, Verselis V, De Zeeuw C, Lee C, Kozak C, Petrasch-Parwez E, Dermietzel R, Willecke K. 2000. Functional expression of the murine connexin 36 gene coding for a neuron-specific gap junctional protein. *J Membr Biol* 176:249–262.
- Thompson RJ, Zhou N, MacVicar BA. 2006. Ischemia opens neuronal gap junction hemichannels. *Science* 312:924–927.
- Trosko J, Chang CC, Wilson M, Upham B, Hayashi T, Wade M. 2000. Gap junctions and the regulation of cellular functions of stem cells during development and differentiation. *Methods Mol Med* 20:245–264.
- Vogt A, Hormuzdi SG, Monyer H. 2005. Pannexin1 and Pannexin2 expression in the developing and mature rat brain. *Mol Brain Res* 141:113–120.
- Wang HL, Chang WT, Yeh TH, Wu T, Chen MS, Wu CY. 2004. Functional analysis of mutant connexin-32 associated with X-linked dominant Charcot-Marie-Tooth disease. *Neurobiol Dis* 15:361–370.
- White TW. 2002. Unique and redundant connexin contributions to lens development. *Science* 295:319, 320.
- White TW, Wang H, Mui R, Litteral J, Brink PR. 2004. Cloning and functional expression of invertebrate connexins from *Halocynthia* pyriformis. *FEBS Lett* 577:42–48.
- Wilcox KS, Dichter MA. 1994. Paired pulse depression in cultured hippocampal neurons is due to a presynaptic mechanism independent of GABA<sub>B</sub> autoreceptor activation. *J Neurosci* 14:1775–1788.
- Willecke K, Eiberger J, Degen J, Eckardt D, Romualdi A, Guldenagel M, Deutsch U, Söhl G. 2002. Structural and functional diversity of connexin genes in the mouse and human genome. *Biol Chem* 383:725–737.
- Yamamura T, Konola JT, Wekerle H, Lees MB. 1991. Monoclonal antibodies against myelin proteolipid protein: Identification and characterization of two major determinants. *J Neurochem* 57:1671–1680.
- Yeh HI, Rothery S, Dupont E, Coppen SR, Severs NJ. 1998. Individual gap junction plaques contain multiple connexins in arterial endothelium. *Circ Res* 83:1248–1263.
- Yum SW, Kleopa KA, Shumas S, Scherer SS. 2002. Diverse trafficking abnormalities for connexin32 mutants causing CMTX. *Neurobiol Dis* 11:43–52.
- Zappala A, Cicero D, Serapide MF, Paz C, Catania MV, Falchi M, Parenti R, Panto MR, La Delia F, Circirata F. 2006. Expression of pannexin1 in the CNS of adult mouse: Cellular localization and effect of 4-aminopyridine-induced seizures. *Neuroscience* 141:167–178.